

# Observation and Analysis of the “Galaxy” Defect in 4H-SiC Through X-Ray Synchrotron Topography

Kaixuan Zhang<sup>1,a\*</sup>, Zeyu Chen<sup>1,b</sup>, Shanshan Hu<sup>1,c</sup>, Jianpei Zhang<sup>1,d</sup>,  
Yuzhuo Li<sup>1,e</sup>, Donglin Wu<sup>1,f</sup>, Haochi Wang<sup>1,g</sup>, Balaji Raghothamachar<sup>1,h</sup>,  
Michael Dudley<sup>1,i</sup> and Andrey Soukhojak<sup>2,j</sup>

<sup>1</sup>Department of Materials Science and Engineering, Stony Brook University, Stony Brook, NY 11794, USA

<sup>2</sup>SK siltron css, 1317 Straits Dr, Bay City, MI 48706, USA

<sup>a</sup>kaixuan.zhang@stonybrook.edu, <sup>b</sup>zeyu.chen@stonybrook.edu, <sup>c</sup>shanshan.hu@stonybrook.edu,  
<sup>d</sup>jianpei.zhang@stonybrook.edu, <sup>e</sup>yuzhuo.li@stonybrook.edu, <sup>f</sup>donglin.wu@stonybrook.edu,  
<sup>g</sup>haochi.wang@stonybrook.edu, <sup>h</sup>balaji.raghothamachar@stonybrook.edu,  
<sup>i</sup>michael.dudley@stonybrook.edu, <sup>j</sup>andrey.soukhojak@sksiltron.com

**Keywords:** 4H-SiC, x-ray topography, defect characterization.

**Abstract.** Silicon carbide (SiC) is valued for high-power and high-frequency devices, but its performance is limited by crystalline defects. We report a newly observed defect arrangement, termed the “galaxy” defect, in wafers from a PVT-grown 6-inch 4° off-axis boule. Optical microscopy revealed dense clusters of micron-sized inclusions, while synchrotron X-ray topography (XRT) showed associated dislocation networks. Transmission synchrotron XRT indicated threading dislocation clusters, and grazing images revealed high densities of basal plane dislocations, deflected Frank partials, and threading-edge-dislocation low-angle grain boundaries (TED-LAGBs). The defect evolved as growth progressed, producing increasingly complex dislocation structures. Based on the observation, we proposed a mechanism for the evolution of the defect involving the generation, evolution, and interaction between the inclusions and dislocations.

## Introduction

Silicon Carbide has gained great interest for its high thermal conductivity, high saturation velocity, and high breakdown voltage and, therefore, its suitability to fabricate high-frequency, high-power electronic devices [1, 2]. It has been applied in various fields, including transportation and communication. However, the longevity and performance of SiC devices are hindered by defects within the substrate and epitaxial material. The observation of defects and understanding of their formation mechanism is critical for the improvement of crystal quality and, therefore, better device performance and production yield [3, 4]. Synchrotron X-ray topography is a widely adopted tool for effectively characterizing the defects within single crystals, revealing the detailed structure of defects via diffraction imaging from a synchrotron X-ray light source. Synchrotron XRT can be performed either in the transmission geometry, where whitebeam X-ray is used and images are taken through the whole wafer thickness and provide an overview of the distribution of defects in the crystal. Grazing incidence geometry XRT, on the other hand, uses monochromatic X-ray to image the top few microns from the sample surface, creating a more detailed image of the intersection of defects with the sample surface.

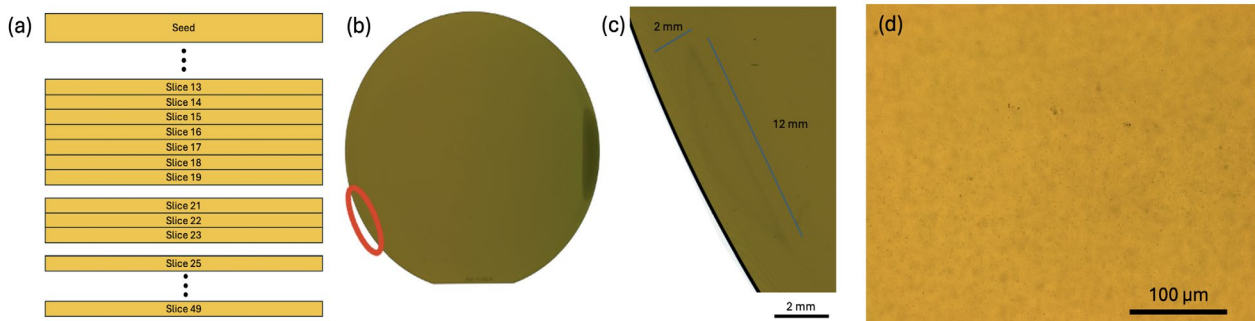
In this study, we report the observation of a new arrangement of defects that we name the “galaxy” defect, which was observed on wafers from the same PVT-grown 6-inch 4° off-axis boule. Optical microscopy images show a region of a highly dense cluster of micrometer-level inclusions. The samples are investigated mainly with a combination of optical microscopy, synchrotron white beam X-ray topography, and grazing-incidence synchrotron X-ray topography. The structure of the “galaxy” defect is revealed, and a model is proposed based on the experimental results and observations.

## Experimental

PVT-grown,  $4^\circ$  off-axis 4H-SiC substrate wafers are characterized by a combination of optical microscopy and synchrotron X-ray topography. XRT images were recorded in both transmission and grazing-incidence geometry. The transmission images were recorded using  $(1\ 1\ -2\ 0)$ ,  $(1\ -1\ 0\ 0)$ , and  $(1\ -1\ 0\ 1)$  reflections using a whitebeam synchrotron source at Beamline 27-HEX at the NSLS-II at Brookhaven National Laboratory. The grazing incidence images were recorded from the Si-face using the  $(1\ 1\ -2\ 8)$  at an energy of 9.1keV at beamline 1-BM of the Advanced Photon Source at Argonne National Laboratory.

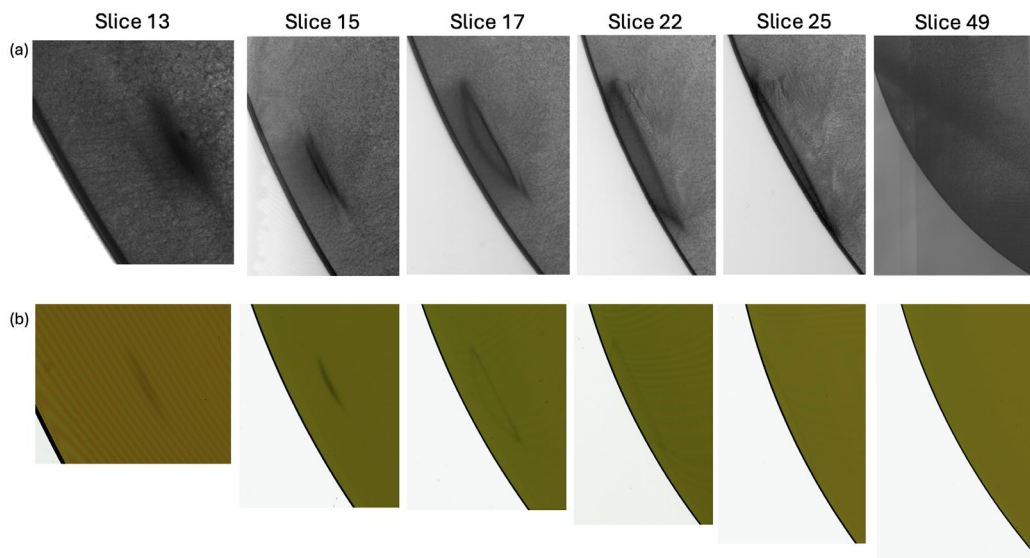
## Results and Discussion

The “galaxy” defect was observed on a series of 150mm PVT-grown  $4^\circ$ -offcut 4H-SiC epitaxial wafers from the same boule from slice 13 to slice 25, as illustrated in Fig. 1(a). They are observed near the edge of the wafer as shown in Fig. 1(b) and Fig. 1(c). Optical microscopy as a cluster of inclusions with diameters of a few microns, as shown in Fig. 1(d).



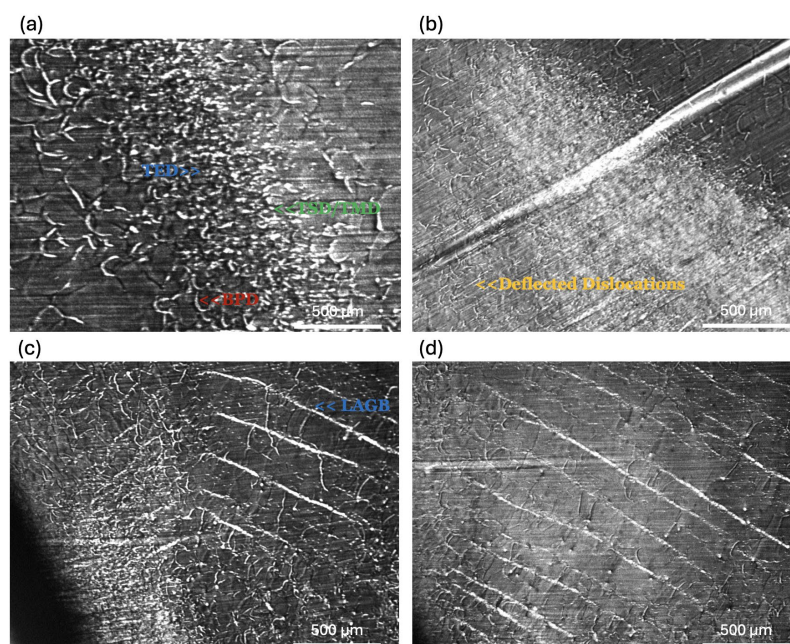
**Fig. 1.** Illustration of the optical observation of the “galaxy” defect, including the location and the wafer numbers and their relevant locations (a); the location of the defect on the boule (b); optical transmission image of the defect on slice 18 (c); and optical transmission microscopy images of the “galaxy defect”.

Fig. 2(a) shows the Transmission XRT, while Fig. 2(b) shows the transmission optical images from the “galaxy” defect region of selected wafers from the boule containing the defect. Transmission XRT images show a dark contrast within the region of the inclusion. Individual defects could not be identified due to the possible high defect density within this region. Also, no individual contrast from the optically observed inclusions could be identified in the topography images. The defect region can be observed to initiate further from the wafer edge and move towards the edge. The cluster can be observed to split into two parts from slice 15. The optical image from slice 49 shows no optical contrast for the defect, while the XRT image shows a large network of prismatic slip dislocations and LAGB as a residual from the defect.



**Fig. 2.** Whitebeam transmission XRT images from  $(1\ 1\ -2\ 0)$  reflection (a) and optical transmission images (b) from slice 13, 15, 17, 22, 25, and 49 showing the evolution of the “galaxy” defect.

Further analysis can also be performed with  $g\cdot b$  analysis, identifying the direction of the Burgers vectors of BPDs in this region. The defect region can be observed to be much darker on the  $(1\ 1\ -2\ 0)$  reflection images compared to the  $(1\ -1\ 0\ 0)$  reflection images. While exact quantitative measurements were difficult due to the high defect density in this region. Qualitatively, around a third of the BPDs in this region are parallel or antiparallel to the step flow direction. Grazing-incidence geometry XRT was performed on the wafer series in order to further identify the defect structure within this region. The results from slice 13, slice 18, slice 25, and slice 49 are selected as representative and shown in Fig. 3. Although the defect density is still too high to investigate the detailed interaction of defects, contrast corresponding to BPD, TED, and TMD can be identified from the grazing image of slice 13. A similar arrangement is observed on the grazing images from slice 18. The density of deflected dislocations is found to be higher on slice 18 compared to slice 13. As the growth proceeds to slice 25, a large LAGB network can be observed to form, which corresponds with the observation from the transmission images. The density of deflected dislocations between the inclusion cluster and the wafer edge is also found to increase.



**Fig. 3.** Grazing-incidence XRT images from  $(1\ 1\ -2\ 8)$  reflection from the Si-face of the “galaxy” defect region from slice 13 (a), slice 18 (b), slice 25 (c), and slice 49 (d).

Further SEM and Raman spectroscopy were used to investigate the composition and origin of the inclusions. However, neither SEM nor Raman spectroscopy was able to identify contrast on the sample surface. Reflective optical microscopy was also not able to resolve any inclusion on the sample surface. The interaction thickness of these characterization methods might have been too low to intersect with any of the inclusions. These inclusions could be due to the transportation of carbon or SiC particles from the source material to the growth interface by drag and thermophoretic forces [5]. However, the exact identity and the origin of the inclusions related to the “galaxy” defect are still under investigation with planned TEM studies.

Based on the observations and XRT images, a model can be proposed for the formation and inclusion of the “galaxy” defect, as illustrated in Fig. 4. Previous studies have shown that TSD/TMD pairs could originate from inclusions during epitaxial growth [6, 7]. A high density of inclusions was observed inside the “galaxy” defect region, which would cause the generation of TSD/TMD pairs and therefore the high density of TSD/TMDs observed on the grazing images. As the location of the “galaxy” defect is very close to the wafer edge, the surface curvature in this area would be comparably high, which would promote the formation of macrosteps during the epitaxial process [8, 9]. These macrosteps could then deflect the TSD/TMDs into frank partials and possible stacking faults, which could be the cause of the high density of deflected dislocations between the inclusion region and the wafer edge [10].

The high density of inclusions in this region could also be the origin of the high density of TEDs. While the generation of TEDs is also possible near inclusions, the prismatic slip dislocation network near the “galaxy” suggests that the slipping of prismatic slip dislocations could also be a contributing factor to the TEDs in this region [8, 11, 12]. The inclusions in these regions could also serve as blockages of the slipping of prismatic slips dislocations, causing them to re-propagate as TED and pile up near the “galaxy” defect region. It is then possible for the high density of TEDs from the prismatic slips with the same orientation to align themselves along the most energetically favorable arrangement, which would explain the formation of TED-LAGB as growth progresses [13]. In the meantime, the inclusions can also serve as pinning points for the movement of BPDs. Both the inclusions and the highly dense TSD/TMDs within this region could serve as pinning points for the movements of BPDs. This pinning effect could cause the multiplication of BPDs in this region via the Frank-Read source, providing a possible explanation for the high BPD density in this region [14].

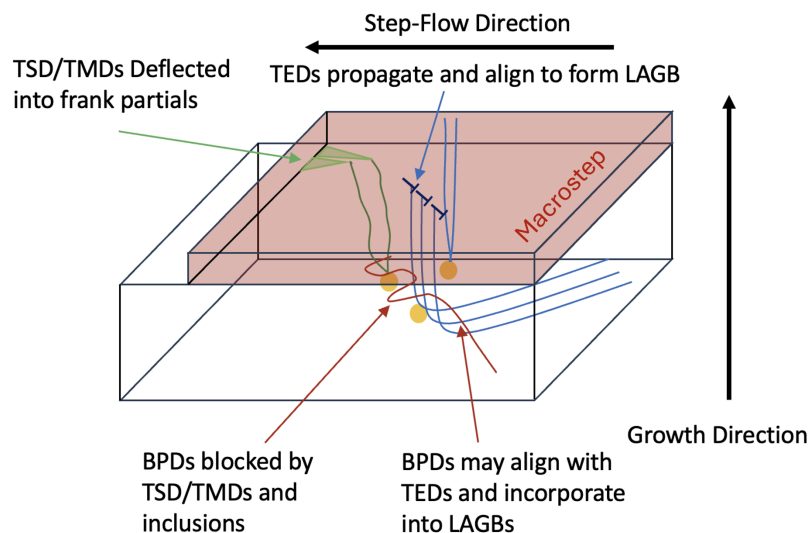


**Fig. 4.** Illustration of the proposed model for the “galaxy” defect based on experimental results and observations.

## Summary

In this study, we investigated a new defect arrangement in PVT-grown 4H-SiC wafer named “galaxy” defect, which was initially observed as micron-level inclusions. The defect arrangements within the

defect are revealed through a combination of optical microscopy, whitebeam synchrotron X-ray topography, and grazing incidence synchrotron topography. A model for the evolution of the defect is proposed based on the experimental results, where the inclusions serve as the origin of TSD/TMDs while also piling up TEDs by blocking prismatic slips and eventually forming TED-LAGB. The inclusions and the TSD/TMDs could be the pinning points causing the multiplication of BPDs in this region. The identification and characterization of the “galaxy” defect provides insights into defect interactions in SiC, which is essential for the improvement of the PVT process in producing 4H-SiC wafers with better quality.

### Acknowledgement

This research was supported by SK siltron css. This research used resources of the Advanced Photon Source (Beamline 1-BM), a U.S. Department of Energy (DOE) Office of Science User Facility operated for the DOE Office of Science by Argonne National Laboratory under Contract No. DE-AC02-06CH11357. The Joint Photon Sciences Institute at SBU provided partial support for travel and subsistence at the Advanced Photon Source. This research used beamline 27-HEX of the National Synchrotron Light Source II, a U.S. Department of Energy (DOE) Office of Science User Facility operated for the DOE Office of Science by Brookhaven National Laboratory under Contract No. DE-SC0012704.

### References

- [1] Dhanaraj, G., B. Raghothamachar, and M. Dudley, Growth and Characterization of Silicon Carbide Crystals, in Springer Handbook of Crystal Growth, G. Dhanaraj, et al., Editors. 2010, Springer Berlin Heidelberg: Berlin, Heidelberg. p. 797-820.
- [2] Codreanu, C., et al., Comparison of 3c SiC, 6h SiC and 4H SiC MESFETs performances. Materials Science in Semiconductor Processing, 2000. 3: p. 137-142.
- [3] St. G. Müller et al., Defects in SiC substrates and epitaxial layers affecting semiconductor device performance, The European Physical Journal Applied Physics, vol. 27, no. 1-3, p.29-35.
- [4] Tsunenobu Kimoto and Heiji Watanabe, Defect engineering in SiC technology for high-voltage power devices. Applied Physics Express, 2020. 13: p. 120101-1-3.
- [5] Z. Wang, Z. Wu, M. Ge, H. Bao, Z. Ma, J. Wu, Study on Carbon Particle Inclusions during 4H-SiC Growth by Using Physical Vapor Transport System, Materials Science Forum, 954 (2019), 46-50.
- [6] D. Hofmann, E. Schmitt, M. Bickermann, M. Kölbl, P.J. Wellmann, A. Winnacker, Analysis on defect generation during the SiC bulk growth process, Materials Science and Engineering: B, 61-62 (1999), 48-53.
- [7] M. Dudley, X. R. Huang, W. Huang, A. Powell, S. Wang, P. Neudeck, M. Skowronski; The mechanism of micropipe nucleation at inclusions in silicon carbide. Appl. Phys. Lett. 75 (1999) 784–786.
- [8] Shanshan Hu, Yafei Liu, Qianyu Cheng, Zeyu Chen, Xiao Tong, Balaji Raghothamachar, Michael Dudley, Investigation of defect formation at the early stage of PVT-grown 4H-SiC crystals, Journal of Crystal Growth, 628 (2024), 127542.
- [9] M. Dudley, F. Wu, H. Wang, S. Byrappa, B. Raghothamachar, G. Choi, S. Sun, E. K. Sanchez, D. Hansen, R. Drachev, S. G. Mueller, M. J. Loboda; Stacking faults created by the combined deflection of threading dislocations of Burgers vector  $c$  and  $c+a$  during the physical vapor transport growth of 4H-SiC. Appl. Phys. Lett. 98 (2011), 232110.

- 
- [10] S. Hu, B. Raghathamachar, Z. Chen, K. Kayang, D. Gersappe, M. Dudley, V. Torres, D. Dukes, D. Lang, A. Martin, H. Briccetti, S. Griswold, T. Kegg, and N. Griffin, New Insights into the Occurrence of Prismatic Slip during PVT Growth of SiC Crystals, *Materials Science Forum*, 1156 (2025), 57-64.
- [11] J. Guo, Y. Yang, B. Raghathamachar, J. Kim, M. Dudley, G. Chung, E. Sanchez, J. Quast, and I. Manning, Prismatic Slip in PVT-Grown 4H-SiC Crystal, *Journal of Electronic Materials*, 46 (2017), 2040-2044.
- [12] Q. Shao, W. Geng, S. Xu, P. Chen, X. Zhang, R. Shen, H. Tian, X. Pi, D. Yang, and R. Wang, Nucleation of Threading Dislocations in 4H-SiC at Early Physical-Vapor-Transportation Growth Stage, *Crystal Growth and Design* (2023), 5204-5210.
- [13] Q. Cheng, Z. Chen, S. Hu, B. Raghathamachar, M. Dudley, Analysis of Threading Edge Dislocation Low-Angle Grain Boundary Network Distributions in 4H-SiC Wafers Through Synchrotron X-ray Topography and Ray-Tracing Simulation. *J. Electron. Mater.* 54 (2025), 5037-5050.
- [14] H. Wang, F. Wu, S. Byrappa, B. Raghathamachar, M. Dudley, P. Wu, I. Zwieback, A. Souzis, G. Ruland, T. Anderson, Synchrotron topography studies of the operation of double-ended Frank–Read partial dislocation sources in 4H-SiC, *Journal of Crystal Growth*, 401 (2014), 423-430.